

## Phase transformation and thermal expansion of Cu/ZrW<sub>2</sub>O<sub>8</sub> metal matrix composites

Hermann Holzer<sup>a)</sup> and David C. Dunand<sup>b)</sup>

*Department of Materials Science and Engineering, Massachusetts Institute of Technology, Cambridge, Massachusetts 02139*

(Received 5 February 1998; accepted 15 July 1998)

Powder metallurgy was used to fabricate fully dense, unreacted composites consisting of a copper matrix containing 50–60 vol% ZrW<sub>2</sub>O<sub>8</sub> particles with negative thermal expansion. Upon cycling between 25 and 300 °C, the composites showed coefficients of thermal expansion varying rapidly with temperature and significantly larger than predicted from theory. The anomalously large expansion on heating and contraction on cooling are attributed to the volume change associated with the allotropic transformation of ZrW<sub>2</sub>O<sub>8</sub> between its high-pressure  $\gamma$ -phase and its low-pressure  $\alpha$ - or  $\beta$ -phases. Based on calorimetry and diffraction experiments and on simple stress estimations, this allotropic transformation is shown to result from the hydrostatic thermal stresses in the particles due to the thermal expansion mismatch between matrix and reinforcement.

### I. INTRODUCTION

Metal matrix composites are attractive materials for applications where the high thermal conductivity of metals and the low thermal expansion of ceramics are simultaneously needed, e.g., in electronics heat sinks with high heat dissipation and low thermal expansion mismatch with the silicon chip or its alumina substrate.<sup>1</sup> Because increasing the ceramic content of a composite decreases both its thermal expansion and its thermal conductivity, ceramics with as low a thermal expansion as possible are desirable to maximize the conductivity-expansion ratio of the composite.<sup>2,3</sup> A composite such as Cu/ZrW<sub>2</sub>O<sub>8</sub>,<sup>4</sup> consisting of a high-conductivity metallic matrix and ceramic phase with a strongly negative coefficient of thermal expansion (CTE), is thus ideally suited for electronics thermal management applications, and may also exhibit an isotropic zero CTE at high ceramic fractions, for applications in metrology, precision optics, and space structures.

The negative CTE of ZrW<sub>2</sub>O<sub>8</sub> was first measured between 50 and 650 °C by dilatometry and x-ray diffraction by Martinek and Hummel,<sup>5</sup> and was recently confirmed to exist in the temperature range –273 to 777 °C by dilatometry and neutron diffraction by Sleight and co-workers.<sup>6–8</sup> The physical explanation for this unusual behavior is based on a steric contraction on heating due to polyhedra tilting which overweighs the usual chemical bond thermal expansion.<sup>6–10</sup> Compared to other

ceramics with negative CTE,<sup>6,11</sup> ZrW<sub>2</sub>O<sub>8</sub> exhibits a CTE with a unique combination of properties: (i) spatial isotropy due to its cubic structure<sup>8</sup>; (ii) very large magnitude ( $\alpha = -8.7 \times 10^{-6} \text{ K}^{-1}$  for –273 to 420 °C<sup>7</sup>); and (iii) exceptionally broad temperature range of existence (–273 to 777 °C<sup>7</sup>). ZrW<sub>2</sub>O<sub>8</sub> is thermodynamically stable only over a narrow temperature range near 1125 °C, but, after quenching, it is metastable up to 1050 °C, where it decomposes into ZrO<sub>2</sub> and WO<sub>3</sub>.<sup>12,13</sup> Furthermore, ZrW<sub>2</sub>O<sub>8</sub> undergoes a reversible order-disorder transformation at 155 °C<sup>7</sup> from its metastable, low-temperature, cubic  $\alpha$ -phase to a metastable, high-temperature, cubic  $\beta$ -phase, which exhibits a CTE with a smaller magnitude ( $\alpha = -4.9 \times 10^{-6} \text{ K}^{-1}$ ). Also, when subjected to hydrostatic pressure at ambient temperature, the cubic  $\alpha$ -phase transforms to an orthorhombic, high-pressure  $\gamma$ -phase with an even larger, but still negative, CTE value ( $\alpha = -1.0 \times 10^{-6} \text{ K}^{-1}$ ): this transformation initiates below 200 MPa and is essentially complete at 400 MPa.<sup>8</sup> When the pressure is released at ambient temperature,  $\gamma$ -ZrW<sub>2</sub>O<sub>8</sub> remains metastable and is reconverted to cubic  $\alpha$ -ZrW<sub>2</sub>O<sub>8</sub> by heating at 120 °C at ambient pressure.<sup>8</sup>

In the present study, we investigate Cu/ZrW<sub>2</sub>O<sub>8</sub> composites for applications where low thermal expansion and high thermal conductivity are simultaneously desirable. Processing issues are first addressed, in view of the difficulties reported earlier for fabrication of dense, unreacted Cu/ZrW<sub>2</sub>O<sub>8</sub> composites.<sup>4</sup> The thermal expansion properties of the composites are then presented and discussed in the light of the thermal expansion mismatch between matrix and reinforcement, the resulting internal stresses, and the pressure-induced transformation of ZrW<sub>2</sub>O<sub>8</sub>.

<sup>a)</sup>Currently with Electrovac GesmbH, Aufeldgasse 37-39, A-3400 Klosterneuburg, Austria.

<sup>b)</sup>Currently with Department of Materials Science and Engineering, Northwestern University, Evanston, Illinois 60208.

## II. EXPERIMENTAL PROCEDURES

Copper powders (99.5% pure, with size between 45 and 63  $\mu\text{m}$ , from Cerac Inc., Milwaukee, WI) and  $\alpha$ -ZrW<sub>2</sub>O<sub>8</sub> powders (from Wah Chang, Albany, OR), crushed and sieved to match the size of the copper powders, were blended for 2 h in air in a rotary mill. To obtain samples for heat-treatment studies, powder blends with 50 vol% ceramics were compacted by uniaxial cold-pressing in a steel die (12.7 mm in diameter) at 172 MPa followed by cold-isostatic-pressing (CIP) at room temperature under pressures of 275 and 690 MPa.

Dense composite samples were obtained by three routes. First, blended powders with 50 vol% ZrW<sub>2</sub>O<sub>8</sub> were vacuum hot-pressed in a steel die under a uniaxial pressure of 1.4 GPa at 250 °C for 13 h. Second, powder blends with 50 vol% ZrW<sub>2</sub>O<sub>8</sub> were mechanically alloyed in a SPEX mill under argon for 4 h, using an alumina container and alumina balls with a ball-powder ratio of unity. The powders were subsequently hot-pressed under the same conditions as above. Third, copper-coated ceramic particulates were subjected to hot isostatic pressing (HIP) in a copper-lined steel can at 500 °C for 3 h under a pressure of 100 MPa. The ceramic powders were coated with about 2  $\mu\text{m}$  copper (Fig. 1) using standard electroless techniques described

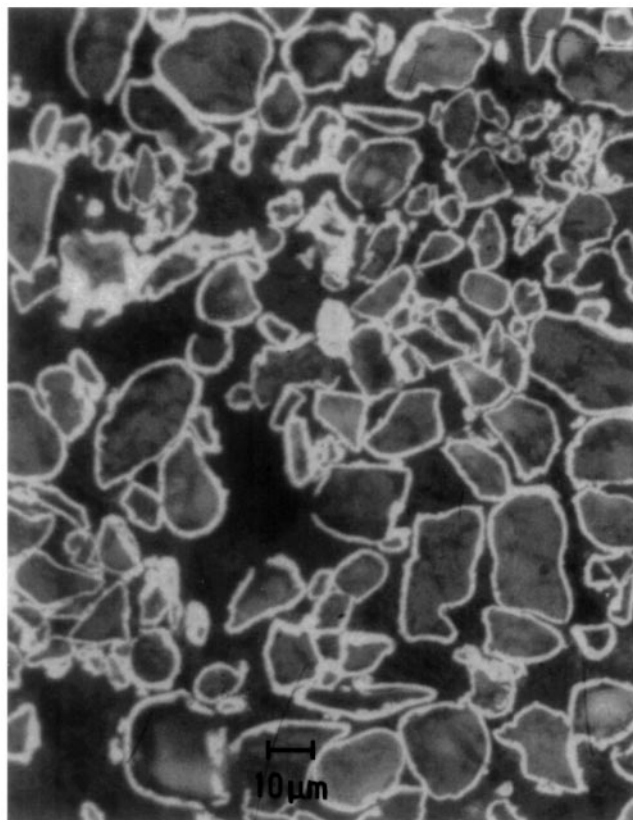


FIG. 1. Optical micrograph of copper-coated ZrW<sub>2</sub>O<sub>8</sub> powders.

in Ref. 14 and plating solutions from Fidelity Chemical Products Corp. (Newark, NJ). All the copper introduced into the composite originated from the electroless deposition, resulting in a ZrW<sub>2</sub>O<sub>8</sub> volume fraction of 60 vol%. In the following, we refer to the three densified composite as hot-pressed, mechanically alloyed, and hot-isostatically pressed, respectively.

X-ray diffraction (XRD) was performed on a Rigaku Rotaflex x-ray diffractometer using Cu K $\alpha$  radiation in air at ambient temperature and under vacuum at elevated temperature. Thermal expansion was measured on composites rods (9 mm in diameter and about 10 mm in length) with a Bahr DIL 801 dilatometer under argon atmosphere with heating/cooling rates of 2 K/min and holding times on heating of 15 min at 100, 200, and 300 °C. Differential scanning calorimetry was performed under argon at the same rates, but without holding times with a DuPont 2100 Calorimeter. Metallographic specimens were mounted in epoxy, ground on SiC paper (300, 800, 1200, and 4000 grit), and polished with 1  $\mu\text{m}$  diamond paste.

## III. RESULTS

### A. Processing

Cold-pressed preforms exhibited densification of about 70% after uniaxial pressing and up to 90% after CIP, but showed only green strength. XRD spectra indicated that after CIP,  $\alpha$ -ZrW<sub>2</sub>O<sub>8</sub> had been partially transformed to high-pressure  $\gamma$ -ZrW<sub>2</sub>O<sub>8</sub>. Vacuum annealing of a green preform at 400 °C for 15 min reconverted ZrW<sub>2</sub>O<sub>8</sub> to its  $\alpha$ -phase, but did not result in significantly higher densities, even after 1 h at temperature.

Because of the chemical reaction reported to occur between copper and zirconium tungstate for typical HIP conditions for copper<sup>4</sup> (600 °C for 3 h, much below the ZrW<sub>2</sub>O<sub>8</sub> vacuum decomposition temperature of 1050 °C<sup>12</sup>), heat-treatment studies were performed to determine a time-temperature processing window for composite densification. High-temperature XRD investigations of loose, mixed powders showed no reaction between Cu and ZrW<sub>2</sub>O<sub>8</sub> up to 600 °C for short times. The XRD spectra were obtained by heating at a rate of 20 K/min, holding for 1 min at the desired temperature (100, 200, 300, and 600 °C) and performing the measurement for 7.5 min under vacuum. The  $\alpha$ - $\beta$  phase transformation was observed in these spectra, as indicated by the disappearance of the (221), (310), (410), and (422) peaks between 100 and 200 °C. The spectrum at 600 °C also showed the onset of a reaction between metal and ceramic, confirming results obtained at this temperature after 3 h in Ref. 4.

Heat-treatment studies on cold-isostatically pressed preforms were done in vacuum between 300 and 700 °C. Significant reaction between Cu and ZrW<sub>2</sub>O<sub>8</sub> was ob-

served only for the heat treatments at 600 and 700 °C, where the major peaks of ZrW<sub>2</sub>O<sub>8</sub> vanished. Figure 2 summarizes the time-temperature processing window for these Cu/ZrW<sub>2</sub>O<sub>8</sub> composites. Some heat treatments were repeated with fully densified samples with the same

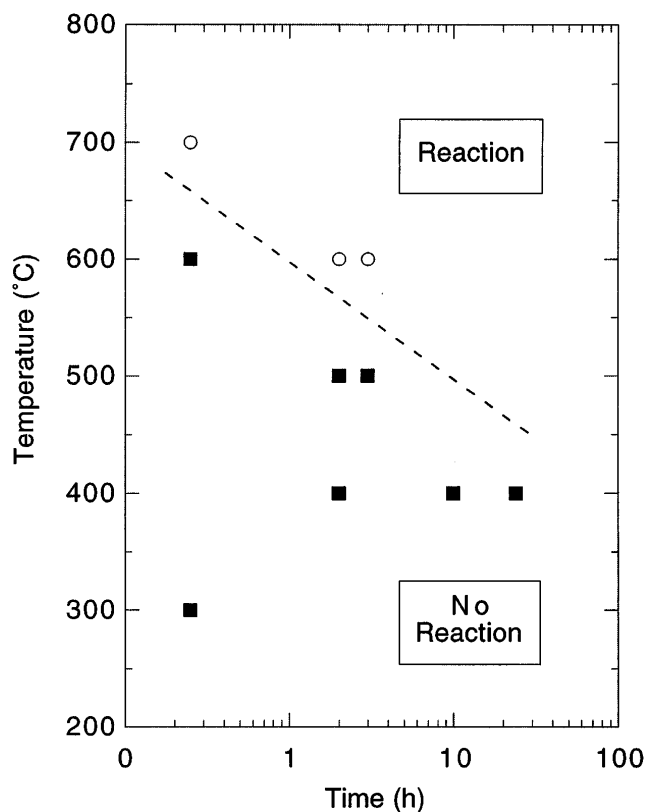


FIG. 2. Processing window for Cu/ZrW<sub>2</sub>O<sub>8</sub> composites (measurements done in vacuum on cold-isostatically pressed preforms).

results. XRD spectra of specimens heat treated at 400 and 500 °C for 1 h under hydrogen again showed no indication of reaction between the two phases.

Metallography of the hot-pressed composite [Fig. 3(a)] shows that the ceramic phase is quite uniformly distributed in the copper matrix and that little porosity exists. The measured density is 6.96 g/cm<sup>3</sup>, corresponding to apparent porosities between 0.8 and 2.8%. These bounds were calculated from theoretical densities of a composite containing 50 vol% ZrW<sub>2</sub>O<sub>8</sub> in the  $\alpha$ -phase and  $\gamma$ -phase, respectively, using densities at 20 °C for Cu (8.96 g/cm<sup>3</sup><sup>15</sup>), for  $\alpha$ -ZrW<sub>2</sub>O<sub>8</sub> (5.072 g/cm<sup>3</sup><sup>16</sup>) and for  $\gamma$ -ZrW<sub>2</sub>O<sub>8</sub> (5.355 g/cm<sup>3</sup><sup>16</sup>). Despite the much lower compaction pressure and the higher ceramic content, the composite hot-isostatically pressed from copper-coated particulates [Fig. 3(b)] exhibited a better ceramic distribution and a higher compaction, because the coating prevented all ceramic-ceramic contact points; the density of 6.63 g/cm<sup>3</sup> corresponds to apparent porosities between 0.0 and 2.5% for 60 vol%  $\alpha$ - or  $\gamma$ -ZrW<sub>2</sub>O<sub>8</sub>, respectively. The mechanically alloyed composite exhibited a majority phase consisting of intimate mixture of ceramic and metal [unresolved, gray matrix in Fig. 3(c)], as well as small amounts of unalloyed matrix and particulates [light and dark discontinuous phases in Fig. 3(c)]. The measured density of 7.03 g/cm<sup>3</sup> corresponds to apparent porosities between -0.2 and 1.8% for 50 vol%  $\alpha$ - or  $\gamma$ -ZrW<sub>2</sub>O<sub>8</sub>, respectively. The XRD spectrum of the mechanically alloyed powder showed no peaks for ZrW<sub>2</sub>O<sub>8</sub>, which could result from the amorphization of the ceramic phase or from strong peak broadening due to small crystallite size. After annealing at 400 °C for 1 h, XRD spectra did not show the ZrW<sub>2</sub>O<sub>8</sub> phase,

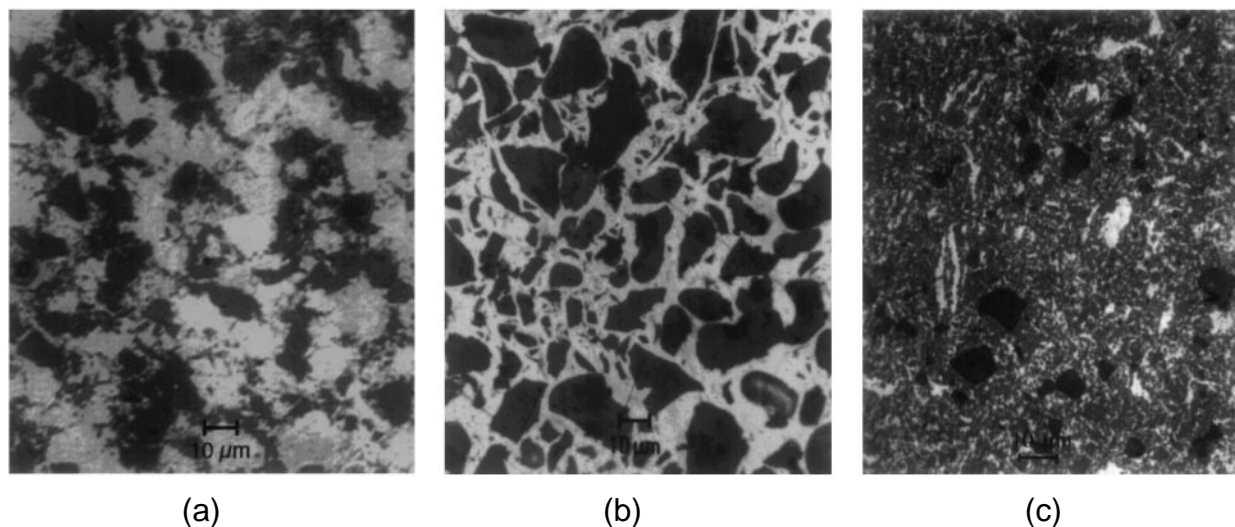


FIG. 3. Optical micrographs of Cu-ZrW<sub>2</sub>O<sub>8</sub> composites (metal is light, ceramic is dark): (a) hot-pressed from blended powders (50 vol% ceramic); (b) hot-isostatically pressed from copper-coated ceramic powders (60 vol% ceramic); (c) hot-pressed from mechanically alloyed powders (50 vol% ceramic). Gray phase consists of a fine, unresolved mixture of metal and ceramic.

but after annealing at 700 °C for 15 min, new XRD peaks indicated that a reaction between copper and ZrW<sub>2</sub>O<sub>8</sub> had occurred.

During the hot compaction of blended, uncoated powders,  $\alpha$ -ZrW<sub>2</sub>O<sub>8</sub> was partially transformed to the high-pressure phase  $\gamma$ -ZrW<sub>2</sub>O<sub>8</sub>, as evidenced by XRD measurements. Because  $\gamma$ -ZrW<sub>2</sub>O<sub>8</sub> has a much higher CTE than  $\alpha$ -ZrW<sub>2</sub>O<sub>8</sub>, it is desirable to induce the  $\gamma$ - $\alpha$  back-transformation, which takes place at 120 °C at ambient pressure according to Ref. 6. To investigate this back-transformation, XRD was performed on the following heat-treated samples: (i) 90% dense composite samples, hot-isostatically pressed from blended, uncoated ceramic-metal powders; (ii) 90% dense cold-isostatically pressed preforms; (iii) loose  $\gamma$ -ZrW<sub>2</sub>O<sub>8</sub> powders without copper, obtained by CIP at 690 MPa. The ratios of the areas of the two main diffraction peaks for  $\gamma$ - and  $\alpha$ -ZrW<sub>2</sub>O<sub>8</sub>, i.e.,  $(201)_{\gamma}/(210)_{\alpha}$  and  $(231)_{\gamma}/(211)_{\alpha}$ , respectively, were used as a measure of the fraction of transformed ZrW<sub>2</sub>O<sub>8</sub>. Figure 4 shows that increasing heat-treatment time and/or temperature increases the extent of the  $\gamma$ - $\alpha$  back-transformation, which is mostly complete after 24 h at 400 °C or 2 h at 500 °C, within the window where no reaction is expected (Fig. 2). The compaction state of the samples is also important: whereas nearly no high-pressure  $\gamma$ -phase remained in the mixed powders after 24 h at 400 °C (or in the green composite preforms after 2 h at 500 °C), a significantly higher amount of  $\gamma$ -phase was found in the hot-isostatically pressed sample for the equivalent heat treatments (Fig. 4). This is probably because the back-transformation is mechanically hindered by the copper matrix, which must creep to enable the volume expansion associated with the  $\gamma$ - $\beta$  transformation.

Finally, XRD spectra of composites processed with copper-coated powders exhibited no high-pressure

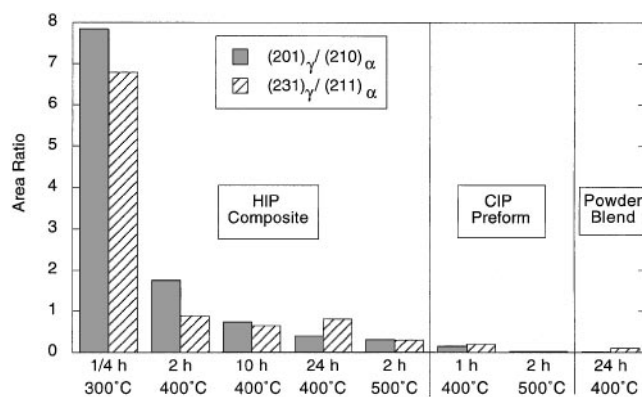


FIG. 4. Ratio of x-ray diffraction peaks areas of the high pressure  $\gamma$ -phase and low pressure  $\alpha$ -phase (for the two main respective peaks) after different heat treatments for a partially compacted hot-isostatically pressed composite, a cold-isostatically pressed preform, and a loose powder blend.

$\gamma$ -phase after HIP. However, some high-pressure  $\gamma$ -phase was found in the composite after thermal cycling, as discussed in more detail later.

## B. Calorimetry

Figure 5 shows the first heating segment of the calorimetric curves of as-received  $\alpha$ -ZrW<sub>2</sub>O<sub>8</sub> powders,  $\gamma$ -ZrW<sub>2</sub>O<sub>8</sub> powders produced by CIP, and the hot-isostatically pressed composite. The  $\gamma$ -ZrW<sub>2</sub>O<sub>8</sub> powders exhibited a narrow peak at 133 °C [peak (1)], a large, broad peak at 290 °C [peak (2)], which was lowered to 270 °C for a lower heating rate of 1 K/min, and three weak, broad peaks near 345, 435, and 480 °C [peaks (3–5)]. These peaks were observed with much lower intensity in  $\alpha$ -ZrW<sub>2</sub>O<sub>8</sub> at 130 °C [peak (1)], 270 °C [peak (2)], 415 °C [peak (4)], and 485 °C [peak (5)]. The composite did not display peak (1) but showed peaks (2) and (3) at 266 and 313 °C, as well as peaks (4) and (5) at temperatures similar to the powders. For the powders, no peaks were observed during the subsequent cooling and a second temperature cycle; the composite exhibited on cooling a very broad signal between 500 and 300 °C, but no peaks during a subsequent cycle.

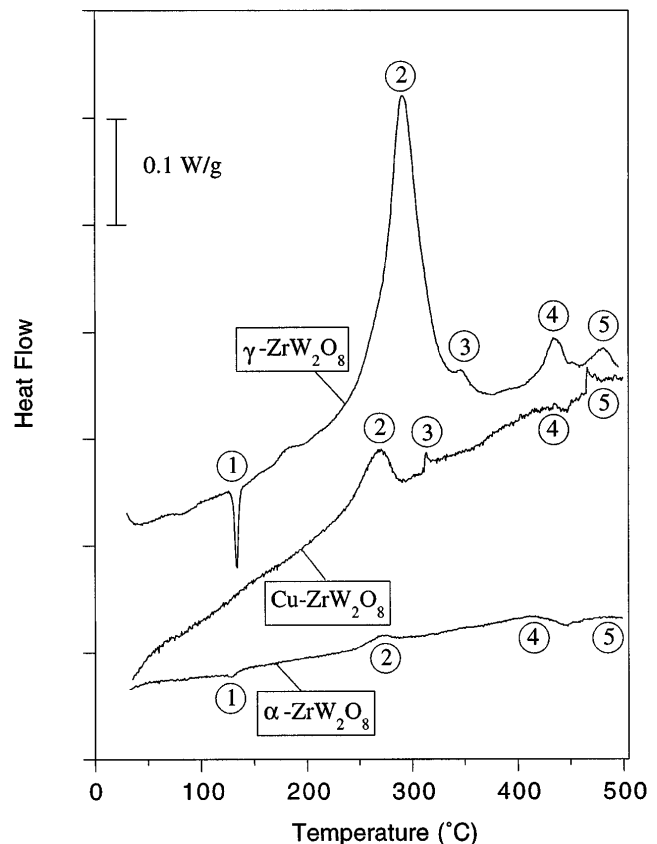


FIG. 5. Calorimetric heating curves for as-received  $\alpha$ -ZrW<sub>2</sub>O<sub>8</sub> powder, cold-isostatically pressed  $\gamma$ -ZrW<sub>2</sub>O<sub>8</sub> powders, and a hot-isostatically pressed Cu/ZrW<sub>2</sub>O<sub>8</sub> composite.

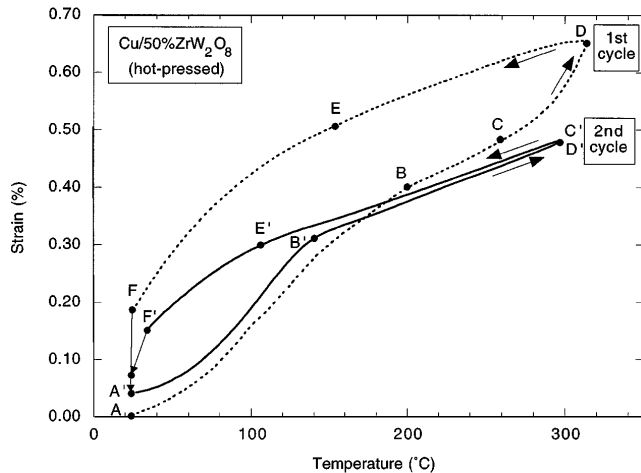


FIG. 6. Dilatometric curves for the hot-pressed composite.

### C. Dilatometry

Figure 6 shows the first two expansion curves of the composite hot-pressed from powder blends and subsequently annealed at 300 °C for 15 min. In the first cycle, the sample expanded strongly up to about 200 °C (point B), and then at a much lower rate up to 260 °C (point C). Upon subsequent heating to 315 °C, a large expansion was again measured to point D. In the cooling section of the first cycle, the CTE slope was low down to about 150 °C (point E), and then again very large up to ambient temperature (point F), where a residual strain of 0.19% was recorded. However, the sample continued shrinking slowly at room temperature, and showed a residual strain of 0.04% (point A') after 48 h. The second cycle in Fig. 6 is qualitatively similar to the first cycle, except for the following differences: the initial large expansion on heating subsided at a lower temperature (point B'), the second large expansion at high temperature was missing (points C' and D' are superimposed), and the large shrinkage on cooling started at a lower temperature (point E'). As for the first cycle, the plastic strain of 0.11% at the end of the second cycle (point F') was recovered almost completely after 48 h, when an additional residual strain of 0.02% was measured. Three subsequent cycles overlapped with the second cycle.

Figure 7 shows for the hot-isostatically pressed composite the first and second thermal expansion curves, which are qualitatively similar to those of the hot-pressed sample (Fig. 6). The first cycle exhibited a very high expansion on heating over the whole temperature range. On cooling, the contraction was initially low, but increased with decreasing temperature, as in Fig. 6. The residual strain (0.29%) was largely recovered after 48 h. We note that the first cycles in Figs. 6 and 7 cannot be directly compared, since the hot-pressed sample, unlike the hot-isostatically pressed sample, had not been subjected to a 300 °C anneal prior to dilatometry, because of the lack

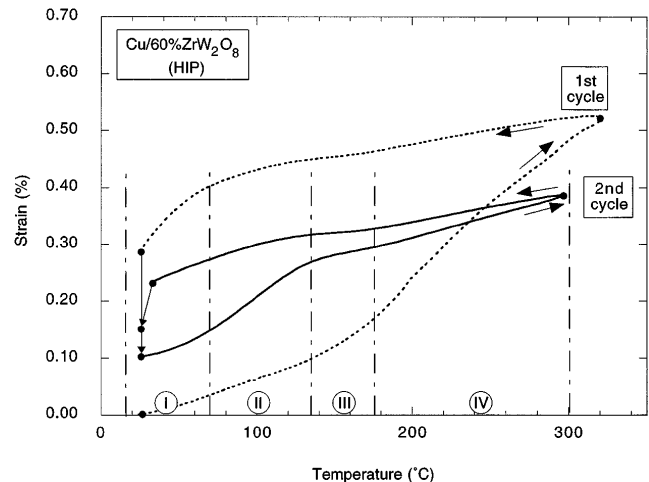


FIG. 7. Dilatometric curves for the hot-isostatically pressed composite.

of XRD evidence of the high-pressure phase. The second cycles for both samples are, however, quite similar and reproducible upon further cycling, indicating that the thermal expansion behavior was stabilized.

Figure 8 shows the first two thermal expansion curves of the mechanically-alloyed composite which was annealed at 300 °C for 15 min prior to testing. Unlike the other composites (Figs. 6 and 7), the first two thermal expansion curves are smooth and reproducible. The small residual strain observed at the end of each cycle (0.05 and 0.03%) was almost fully recovered at ambient temperature in the 48 h interval before the following cycle.

## IV. DISCUSSION

### A. Calorimetry

For all samples, the main peaks for initial heating in Fig. 5 were not observed upon cooling or during subsequent thermal cycles, indicating that the corresponding

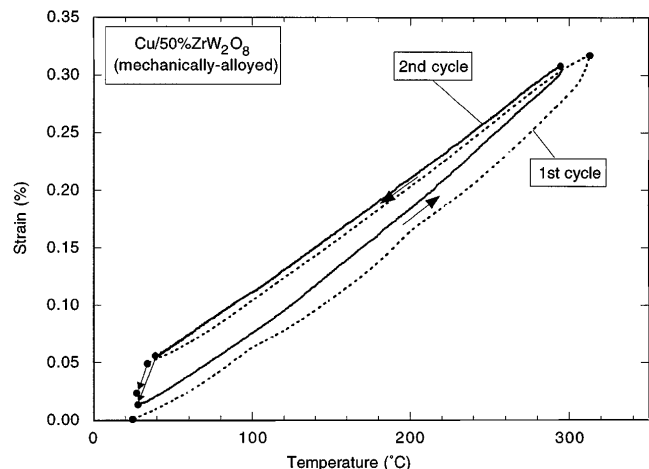


FIG. 8. Dilatometric curves for the mechanically alloyed composite.

phase transformations occur from the metastable  $\gamma$ -phases to the more stable  $\alpha$ - or  $\beta$ -phases (we note that  $\alpha$ -ZrW<sub>2</sub>O<sub>8</sub> is merely the most stable of all metastable phases at ambient temperature and pressure, where the base oxides ZrO<sub>2</sub> and WO<sub>3</sub> are thermodynamically stable<sup>12,13</sup>).

For  $\gamma$ -ZrW<sub>2</sub>O<sub>8</sub>, peak (1) at 133 °C corresponds to the  $\gamma$ - $\alpha$  transformation (measured at 120 °C by Evans *et al.*<sup>6</sup>), while peak (2) at 270–290 °C can be assigned to the  $\gamma$ - $\beta$  transformation, occurring if the  $\gamma$ - $\alpha$  transformation at 133 °C is incomplete for kinetic reasons. The  $\alpha$ - $\beta$  transformation at 155 °C is not observed by calorimetry, as expected for a second-order phase transformation.<sup>17</sup> While the origin of the small peak (3) at 345 °C is unclear, the two small peaks (4–5) are tentatively interpreted as limited oxygen loss from the powder surface reported by Ref. 13. The calorimetric curve for  $\alpha$ -ZrW<sub>2</sub>O<sub>8</sub> shows very weak peaks similar to those for  $\gamma$ -ZrW<sub>2</sub>O<sub>8</sub>, indicating that the as-received  $\alpha$ -powders contain a small amount of  $\gamma$ -phase, estimated as 1% from the ratio of the areas of peak (2).

The hot-isostatically pressed composite shows no  $\gamma$ - $\alpha$  peak (1), while the  $\gamma$ - $\beta$  peak (2) and peak (3) are shifted by 25–30 K as compared to those in the  $\gamma$ -ZrW<sub>2</sub>O<sub>8</sub> powder. Such a shift can be explained by internal mismatch stresses, as discussed in more detail in the following section. The area ratio of peaks (2) gives an approximate 16 vol%  $\gamma$ -phase content in the composite (corresponding to about a quarter of the ceramic content). Peaks (4) and (5) match roughly the corresponding peaks in the powders and could also be due to oxygen loss from the ceramic. The lack of peaks on cooling and subsequent cycling, which are expected from mismatch stresses as discussed in the following paragraph, is explained by the very small sample size (about 1 mm<sup>3</sup>), which probably did not allow the buildup of internal stresses necessary for the formation of the high-pressure  $\gamma$ -phase upon cooling.

## B. Composite residual stresses

Because of the very large CTE mismatch between Cu and  $\alpha$ -ZrW<sub>2</sub>O<sub>8</sub> ( $\Delta\alpha = 29 \times 10^{-6} \text{ K}^{-1}$  at ambient temperature), significant residual stresses exist at ambient temperature after cooling from the fabrication temperature, where the composite is assumed to be free of thermal mismatch stresses. Since copper exhibits a low yield stress, matrix plastic deformation occurs for a small temperature excursion  $\Delta T_p$  upon cooling from the stress-free temperature. An estimate for  $\Delta T_p$  can be found by considering a mismatching sphere in an infinite, elastic, ideally plastic matrix, as treated by Lee *et al.*<sup>18</sup> Matrix plasticity starts at the particle-matrix interface when the particle hydrostatic stress  $p$  reaches two thirds of the matrix yield stress  $\sigma_y$ . The mismatch strain can

then be calculated as<sup>18</sup>:

$$\epsilon = \frac{p}{4 \cdot G \cdot \beta}, \quad (1)$$

where  $G$  is the matrix shear modulus and  $\beta$  is a constant containing the matrix Poisson's ratio and the bulk moduli of the matrix and the particle. Identifying the radial mismatch strain  $\epsilon$  as  $\Delta\alpha\Delta T_p$ , taking a representative matrix yield stress value ( $\sigma_y = 50 \text{ MPa}$ ), and using compressibility for particle and matrix ( $K_{\text{ZrW}_2\text{O}_8} = 69.4 \text{ GPa}^8$  and  $K_{\text{Cu}} = 138 \text{ GPa}^{19}$ ) and matrix shear modulus for Cu ( $G_{\text{Cu}} = 48.3 \text{ GPa}^{19}$ ), the temperature drop for the onset of matrix plasticity predicted by Eq. (1) is  $\Delta T_p = 11 \text{ K}$ . The particle hydrostatic compressive stress is then  $p = 2/3\sigma_y = 33 \text{ MPa}$ .

Using the Eshelby technique,<sup>1</sup> which unlike Eq. (1) is valid for finite fraction of particles, the temperature excursion corresponding to the above particle hydrostatic stress is  $\Delta T_p = 21 \text{ K}$  (assuming a value of 0.3 for the ceramic Poisson ratio and a volume fraction  $v_p = 0.5$ ). It can thus be safely assumed that the matrix is fully plastic at ambient temperature after cooling from the fabrication temperature (250 or 500 °C) or the subsequent annealing temperature (300 °C).

It is unknown whether the high-pressure  $\gamma$ -ZrW<sub>2</sub>O<sub>8</sub> formed during preform CIP transformed to the low-pressure  $\alpha$ - or  $\beta$ -phases upon initial heating to the hot-compaction temperature. During compaction, however, the ZrW<sub>2</sub>O<sub>8</sub> particulates were subjected to compressive hydrostatic pressures on the order of 100 MPa (HIP) and 1.4 GPa (hot pressing). By comparison, Evans *et al.*<sup>8</sup> reported that an equilibrium mixture of 36%  $\gamma$ -ZrW<sub>2</sub>O<sub>8</sub> and 64%  $\alpha$ -ZrW<sub>2</sub>O<sub>8</sub> exists at ambient temperature for an hydrostatic stress of 200 MPa, and that the transformation is complete for a stress of 400 MPa. In the absence of a pressure-temperature phase diagram for ZrW<sub>2</sub>O<sub>8</sub>, it is thus reasonable to assume that the hot-pressing pressure of 1.4 GPa was sufficient to fully transform the ceramic to the  $\gamma$ -phase at the fabrication temperature. Furthermore, upon subsequent cooling from that temperature, thermal mismatch stresses produced an additional compressive hydrostatic stress in the particulates, which can be estimated from an expression derived by Lee *et al.* [Eqs. (28) and (29) in Ref. 18], assuming plastic relaxation of the matrix. Using the above materials parameters and assuming a temperature drop of 477 K from the HIP temperature to ambient temperature, the particulates hydrostatic compressive stress due to thermal mismatch is 166 MPa. Furthermore, additional compressive residual stresses are induced in the particulates upon release of the processing pressure, since the bulk modulus of ZrW<sub>2</sub>O<sub>8</sub> is lower than that of copper.

We thus conclude that both hot-pressed and hot-isostatically pressed specimens are likely to exhibit sig-

nificant amounts of high-pressure  $\gamma$ -ZrW<sub>2</sub>O<sub>8</sub> after fabrication at ambient temperature and pressure. The XRD measurements indeed indicate that most of the ceramic in the hot-pressed composite exists in the  $\gamma$ -phase. Because of the lower hydrostatic pressure used during consolidation and the absence of contact points between ceramic particulates due to the copper coating [Figs. 3(a) and 3(b)], the hot-isostatically pressed composite is expected to have less  $\gamma$ -phase than the hot-pressed sample. Unexpectedly, the XRD spectra of the hot-isostatically pressed composite showed a total lack of  $\gamma$ -phase. We believe that this is due to the very shallow penetration depth of x-rays in the specimen surface, where relaxation produced by the free surface and/or sample cutting triggered the  $\gamma$ - $\alpha$  back-transformation which was complete in the hot-isostatically pressed composite because of its lower initial  $\gamma$ -phase content. The  $\gamma$ -phase content of 16 vol% estimated above from calorimetric peak ratios for the hot-isostatically pressed sample is thus more representative of the bulk  $\gamma$ -phase content for that sample.

While unconstrained  $\gamma$ -ZrW<sub>2</sub>O<sub>8</sub> transforms to the  $\alpha$ -phase at 133 °C at ambient pressure (Fig. 5), thermal mismatch in the composite induces tensile hydrostatic stresses in  $\gamma$ -ZrW<sub>2</sub>O<sub>8</sub> particles upon heating the composites from ambient temperature (e.g., in the dilatometry experiments). An estimate for the onset of matrix plasticity is again given by the above calculation, using  $2\Delta T_p = 22$ – $42$  K due to the initial compressive residual stress in the particles. Similarly, upon cooling during the dilatometry experiments, compressive stresses are again induced after a temperature drop of  $\Delta T_p$  (if relaxation leads to a stress-free composite) to  $2\Delta T_p$  (without relaxation).

### C. Dilatometry

Many models based on elastic interactions between matrix and reinforcement give bounds for the CTE of composites, as reviewed in Ref. 20. The most used bounds are those of Turner<sup>21</sup> and Schapery.<sup>22</sup> Turner expression gives an upper bound as:

$$\alpha_T = \frac{v_m \cdot \alpha_m \cdot K_m + v_p \cdot \alpha_p \cdot K_p}{v_m \cdot K_m + v_p \cdot K_p}, \quad (2)$$

where  $v$  is the volume fraction,  $\alpha$  is the CTE,  $K$  is the bulk modulus, and the subscripts  $m$  and  $p$  are for matrix and particle, respectively. Schapery's lower bound is

$$\alpha_s = v_m \alpha_m + v_p \alpha_p + \frac{4G_p}{K_c} \frac{v_m(\alpha_p - \alpha_m)(K_c - K_m)}{3K_m + 4G_p}, \quad (3)$$

where  $K_c$  is the composite modulus given by

$$K_c = \frac{\frac{v_p K_p}{3K_p + 4G_m} + \frac{v_m K_m}{3K_m + 4G_m}}{\frac{v_p}{3K_p + 4G_m} + \frac{v_m}{3K_m + 4G_m}}. \quad (4)$$

Inverting the subscripts  $m$  and  $p$  in Eq. (3) gives Schapery's upper bound, which is lower than Turner's expression [Eq. (2)] and corresponds to the bound derived by Kerner.<sup>23</sup> Since for Cu/ZrW<sub>2</sub>O<sub>8</sub> composites both the bulk modulus and the thermal expansion are larger for the matrix than for the particles, Eq. (2) is an upper bound while Eq. (3) is a lower bound. This is the opposite of the case for most metal matrix composites examined to date, where the metallic matrix has a higher thermal expansion but a lower bulk modulus than the ceramic reinforcement. For the same reason, the bounds given by Eq. (2) and (3) are higher than the rule of mixture value. Table I gives the CTE for Cu/ZrW<sub>2</sub>O<sub>8</sub> composites calculated from Eqs. (2) and (3), using an average CTE for copper in the temperature interval of interest, the CTE of the three ZrW<sub>2</sub>O<sub>8</sub> phases determined from literature data, and elastic constants given above.

In the following paragraphs, we discuss the complex dilatometric behavior of Figs. 6–8 based on the CTE bounds given by Eqs. (2) and (3) in Table I and the allotropic volume change of 5%<sup>8</sup> associated with the  $\alpha$ - $\gamma$  phase transformation described in the previous section.

#### 1. Hot-pressed composite

The XRD spectrum after heat treatment at 300 °C but before cycling shows that most of ZrW<sub>2</sub>O<sub>8</sub> exists in the  $\gamma$ -phase. The anomalously high expansion upon initial heating (Fig. 6) can be explained by the  $\gamma$ - $\alpha$  volume expansion of 5%. As expected from Le Chatelier's principle, the hydrostatic tensile stresses produced within the ceramic by the thermal mismatch on heating depresses the allotropic temperature as compared to the value of 133 °C for the unconstrained powder (Fig. 5).

TABLE I. CTE values ( $10^{-6}$  K<sup>-1</sup>) for Cu and ZrW<sub>2</sub>O<sub>8</sub> from literature data and for Cu/ZrW<sub>2</sub>O<sub>8</sub> composites from Eqs. (2) and (3).

ZrW <sub>2</sub> O <sub>8</sub> content (vol %)	$\alpha$ -ZrW <sub>2</sub> O <sub>8</sub> (20–160 °C)		$\beta$ -ZrW <sub>2</sub> O <sub>8</sub> (200–500 °C)		$\gamma$ -ZrW <sub>2</sub> O <sub>8</sub> (20–500 °C)	
	Eq. (2)	Eq. (3)	Eq. (2)	Eq. (3)	Eq. (2)	Eq. (3)
100	-12.0 <sup>a</sup>	-12.0 <sup>a</sup>	-4.5 <sup>b</sup>	-4.5 <sup>b</sup>	-1.0 <sup>c</sup>	-1.0 <sup>c</sup>
60	4.5	1.1	8.8	6.1	10.1	7.8
50	7.3	4.0	11.1	8.4	12.0	9.8
0	17.1 <sup>d</sup>	17.1 <sup>d</sup>	19.0 <sup>d</sup>	19.0 <sup>d</sup>	18.6 <sup>d</sup>	18.6 <sup>d</sup>

<sup>a</sup>Average between  $\alpha = -10.4 \times 10^{-6}$  K<sup>-1</sup> (50–200 °C<sup>5</sup>) and  $\alpha = -13.5 \times 10^{-6}$  K<sup>-1</sup> (25–155 °C<sup>6</sup>).

<sup>b</sup>Average between  $\alpha = -3.4 \times 10^{-6}$  K<sup>-1</sup> (200–500 °C<sup>5</sup>) and  $\alpha = -5.6 \times 10^{-6}$  K<sup>-1</sup> (155–500 °C<sup>6</sup>).

<sup>c</sup>From Ref. 31 from -253 to 27 °C, assumed to be valid up to 500 °C.

<sup>d</sup>Temperature average from Ref. 31.

The transformation occurs over a large temperature interval (between points A and B, Fig. 6), probably because the volume expansion of the ceramic is limited by matrix thermal expansion and matrix creep. Over an interval of about 60 K between points B and C, the composite CTE ( $\alpha = 12.5 \times 10^{-6} \text{ K}^{-1}$ ) is reduced but still higher than the upper bound (Table I). Between points C and D, a large composite expansion occurs again, most probably as the  $\gamma$ - $\beta$  transformation occurs within the creeping matrix. Upon cooling from point D to E, the Cu/ $\beta$ -ZrW<sub>2</sub>O<sub>8</sub> composite shows a CTE ( $\alpha = 10 \times 10^{-6} \text{ K}^{-1}$ ) within the bounds given by Eqs. (2) and (3). At point E, the  $\beta$ - $\gamma$  transformation (and, at lower temperature, the  $\alpha$ - $\gamma$  transformation) occurs with a concomitant volume contraction of 5%, resulting in a large shrinkage of the composite down to point F. Again, as expected from Le Chatelier's principle, the onset of this transformation occurs at a higher temperature than the equilibrium value of 133 °C, since the thermal mismatch between matrix and particulates produces a compressive hydrostatic stress within the ceramic. The  $\alpha$ - $\gamma$  transformation occurs continuously at a sluggish rate at ambient temperature during the 48 h following the first cycle, as illustrated by the shrinkage between points F and A'.

The differences noted in the second cycle in Fig. 6 (smaller anomalous expansion and shrinkage) indicate that less  $\gamma$ -phase was present at the onset of that cycle. The observation that the three subsequent cycles overlapped with the second cycle confirms that the reversible transformation  $\alpha, \beta \leftrightarrow \gamma$  induced by internal mismatch stresses is indeed responsible for the anomalous composite expansion and contraction.

Other possible reasons for deviation from the elastic bounds given by Eqs. (2) and (3) include matrix plasticity, matrix voids, interfacial delamination, particle fracture, and residual stresses.<sup>24–29</sup> However, none of these mechanisms can satisfactorily explain the unusual behavior observed in Fig. 6: combination of low and high thermal expansion regions, heating-cooling hysteresis, time-dependent recovery at ambient temperature, and repeatability after the second cycle. In particular, the low CTE values found at high temperature (Fig. 6) indicate that particle and matrix are well bonded, since, in the extreme case of full debonding, a composite exhibits the same CTE as the matrix. Also, residual stresses were further ruled out by an experiment where the particle residual stress state at ambient temperature had been altered to be fully tensile through a thermal excursion to 77 K by immersing the composite into liquid nitrogen. The dilatometric curves showed no difference before and after this cryogenic thermal excursion. We thus conclude that mismatch-induced phase transformation is the only mechanism that can satisfactorily explain the dilatometric curves. However, this explanation is based

on indirect measurement and needs to be confirmed by direct experiments, i.e., neutron diffraction or high-intensity x-ray diffraction as a function of temperatures during a thermal cycle.

## 2. Hot-isostatically pressed composite

The main differences with the hot-pressed composite discussed in the previous paragraph are the much lower hydrostatic pressure used during consolidation and the absence of contact points between ceramic particulates resulting from the copper coating [Figs. 3(a) and 3(b)]; both modifications are expected to reduce the amount of high-pressure  $\gamma$ -ZrW<sub>2</sub>O<sub>8</sub> present at ambient temperature after processing. Figure 7 shows the first and second thermal expansion curves of the hot-isostatically pressed composite, which are qualitatively similar to those of the hot-pressed sample (Fig. 6). The first cycle exhibits a high expansion on heating which is, however, lower than for the hot-pressed composite, Fig. 6, indicating that  $\gamma$ -ZrW<sub>2</sub>O<sub>8</sub> was present but in smaller quantities than for the hot-pressed composite. On cooling, the contraction is initially low [ $\alpha = 4\text{--}5 \times 10^{-6} \text{ K}^{-1}$ , within the bounds given by Eqs. (2) and (3)], but increases at low temperature as for Fig. 6. We again stress that the first cycles in Figs. 6 and 7 cannot be directly compared, since the processing and annealing residual stresses were different.

However, the second cycles in Figs. 6 and 7 are quite similar and are in both cases reproducible upon subsequent cycling, indicating that equilibrium was reached. The heating and cooling segments of the second cycle can be divided into 4 segments for which average CTE values are determined. As shown in Fig. 9 for the hot-isostatically pressed composite, the experimental composite CTE on heating is much higher than the upper bound given by Eq. (2) in regions I and II, somewhat higher than the upper bound in region III (but within limit if some  $\gamma$ -ZrW<sub>2</sub>O<sub>8</sub> exists), and well within bounds in region IV, where  $\beta$ -ZrW<sub>2</sub>O<sub>8</sub> is stable. Similar conclusions can be drawn for cooling, where the CTE is on average lower than on heating, because of the residual strain.

From the residual strain at the end of the cycles ( $\epsilon_r = 0.29\%$  for the first cycle and  $\epsilon_r = 0.13\%$  for the second cycle), the volume fraction  $v_\gamma$  of  $\gamma$ -ZrW<sub>2</sub>O<sub>8</sub> present at ambient temperature can be estimated as

$$v_\gamma = \frac{\epsilon_r}{\frac{1}{3} \frac{\Delta V}{V} \cdot v_p}, \quad (5)$$

where  $\Delta V/V = 5\%$  is the allotropic volume difference. For the first and second cycles of the hot-isostatically pressed composite in Fig. 7, Eq. (5) predicts physically plausible values of  $v_\gamma = 29\%$  and  $v_\gamma = 13\%$ , respectively, which are in broad agreement with the value of 16% estimated from the ratio of calorimetry peaks (3)

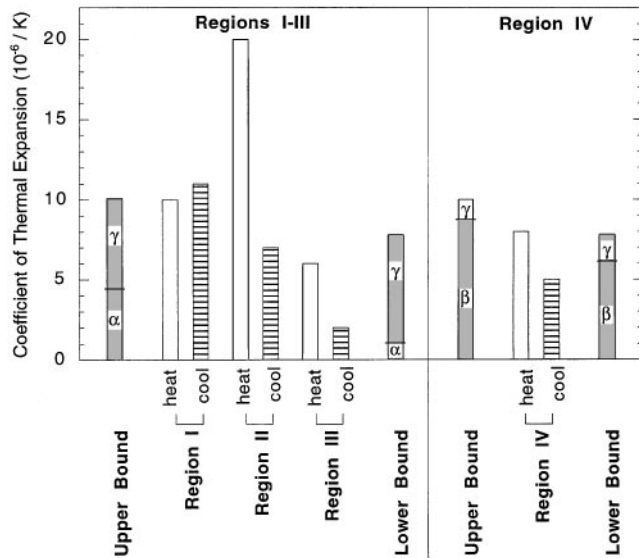


FIG. 9. Comparison between model bounds and measured composite CTE (second, stable cycle of the hot-isostatically pressed Cu/60 vol% ZrW<sub>2</sub>O<sub>8</sub> composite).

in Fig. 5. Similar values ( $v_\gamma = 23\%$  and  $v_\gamma = 13\%$ ) are found for the hot-pressed composite in Fig. 6.

### 3. Mechanically alloyed composite

The mechanically alloyed, hot-pressed composite shows a CTE which increases smoothly from about  $\alpha = 9 \times 10^{-6} \text{ K}^{-1}$  to about  $\alpha = 12 \times 10^{-6} \text{ K}^{-1}$  on heating, and decreases from about  $\alpha = 10 \times 10^{-6} \text{ K}^{-1}$  to about  $\alpha = 9 \times 10^{-6} \text{ K}^{-1}$  on cooling (Fig. 8). These values are for the most part above the upper bound given by Eq. (2), even if all the ceramic exists in the  $\gamma$ -phase (Table I and Fig. 9). While the mechanically alloyed composite shows a smaller residual, recoverable strain at ambient temperature and a much smaller hysteresis below 150 °C than the other composites, it exhibits a larger CTE above 150 °C. As for the other samples, these observations can be explained by the reversible formation of small amounts of  $\gamma$ -ZrW<sub>2</sub>O<sub>8</sub>, possibly in the large, unmixed ZrW<sub>2</sub>O<sub>8</sub> particulates visible in Fig. 3(c). Amorphization or decomposition of ZrW<sub>2</sub>O<sub>8</sub> during mechanical alloying, which is an alternate hypothesis for the high composite CTE, can be ruled out, because the CTE would be much higher than experimentally measured, and because neither hysteresis nor ambient-temperature recovery would occur.

The very small ZrW<sub>2</sub>O<sub>8</sub> particle size in the mechanically alloyed composites thus seems to partially inhibit the formation of the high-pressure  $\gamma$ -phase as compared to the composites with coarser particulates. Two explanations, based on a lower mismatch hydrostatic pressure in the fine particles, can be advanced for

this behavior. First, the mechanically alloyed particles are probably more equiaxed than the as-received particulates [Fig. 3(a)], so that stress concentrations due to thermal mismatch are reduced. Second, plastic relaxation by dislocation punching in the matrix is easier for small particles, because the low number of geometrically necessary dislocation loops per particle reduces or even eliminates strain hardening in the plastic zone.<sup>30</sup>

While mechanical alloying reduces the average composite thermal expansion between 25 and 300 °C and brings us closer to the original goal of a low-expansion Cu/ZrW<sub>2</sub>O<sub>8</sub> composite, this processing route has two major drawbacks: it is time-consuming and thus uneconomical, and it introduces impurities and cold work in the matrix, thus reducing its thermal conductivity. For the simpler route of hot compaction of blended powders, two strategies can be used to limit the undesirable phase transformation leading to the large apparent CTE. First, the mismatch stresses can be reduced by lowering the fabrication pressure and temperature, which is, however, impractical if full densification is to be reached with high volume fractions of ceramics, or the matrix yield stress can be reduced by using very high-purity copper, which is difficult for electroless copper. A second, more promising approach is to alter the chemistry of ZrW<sub>2</sub>O<sub>8</sub> so as to increase the critical pressure for the formation of the  $\gamma$ -phase, for example, through partial or complete replacement of zirconium by hafnium, since  $\alpha$ -HfW<sub>2</sub>O<sub>8</sub> has the same strongly negative CTE value as  $\gamma$ -ZrW<sub>2</sub>O<sub>8</sub>.<sup>6,7</sup>

## V. SUMMARY

Three processing routes were developed to fabricate Cu/ZrW<sub>2</sub>O<sub>8</sub> composites with 50–60 vol% ceramic without reaction and with little or no residual porosity: (i) high-pressure, low-temperature, hot-pressing of blended metal-ceramic powders; (ii) low-pressure, high-temperature, hot-isostatic pressing of copper-coated ceramic powder; and (iii) high-pressure, low-temperature, hot-pressing of mechanically alloyed metal-ceramic powders.

The thermal expansion of the composites was measured between 25 and 300 °C. The first thermal cycle (and to a lesser extent the subsequent thermal cycles) showed hysteresis, time-dependent recovery, as well as coefficients of thermal expansions significantly larger than predicted from composite elastic theory. These effects were reduced in the mechanically-alloyed composites.

This anomalous behavior can be explained by the reversible allotropic transformation of ZrW<sub>2</sub>O<sub>8</sub> between its high-pressure  $\gamma$ -phase and its low-pressure  $\alpha$ - or  $\beta$ -ZrW<sub>2</sub>O<sub>8</sub> phases, which is accompanied by a substantial volume change.

Experimental calorimetry and diffraction measurements as well as theoretical stress estimations show that  $\gamma$ -ZrW<sub>2</sub>O<sub>8</sub> is initially formed by the high isostatic pressure used during processing. Upon subsequent heating and cooling, hydrostatic stresses produced in the particles by the thermal expansion difference between matrix and reinforcement are sufficient to reversibly induce the allotropic transformation. To the best of our knowledge, this is the first time that a phase transformation has been observed in a metal matrix composite as a result of thermal mismatch stresses.

## ACKNOWLEDGMENTS

We acknowledge the sponsorship of the present study by Electrovac GesmbH (Klosterneuburg, Austria). We also thank Dr. John Haygarth from Wah Chang (Albany, OR) for supplying  $\alpha$ -ZrW<sub>2</sub>O<sub>8</sub> powders, Mr. Hank Lajoie from Fidelity Chemicals Products Corp. (Newark, NJ) for supplying electroless plating solutions, and Mr. Brian Elliott from Northwestern University for vacuum hot-pressing of two specimens.

## REFERENCES

1. T. W. Clyne and P. J. Withers, *An Introduction to Metal Matrix Composites* (Cambridge University Press, Cambridge, 1993).
2. M. F. Ashby, *Materials Selection in Mechanical Design* (Pergamon, Oxford, 1992).
3. M. F. Ashby, *Acta Metall. Mater.* **41**, 1313 (1993).
4. C. Verdon and D. C. Dunand, *Scripta Mater.* **36**, 1075 (1997).
5. C. Martinek and F. A. Hummel, *J. Am. Ceram. Soc.* **51**, 227 (1968).
6. J. S. O. Evans, T. A. Mary, T. Vogt, M. A. Subramanian, and A. W. Sleight, *Chem. Mater.* **8**, 2809 (1996).
7. T. A. Mary, J. S. O. Evans, T. Vogt, and A. W. Sleight, *Science* **272**, 90 (1996).
8. J. S. O. Evans, Z. Hu, J. D. Jorgensen, D. N. Argyriou, S. Short, and A. W. Sleight, *Science* **275**, 61 (1997).
9. A. K. A. Pryde, K. D. Hammonds, M. T. Dove, V. Heine, J. D. Gale, and M. C. Warren, *J. Phys. Condens. Matter* **8**, 10973 (1996).
10. A. K. A. Pryde, K. D. Hammonds, M. T. Dove, V. Heine, J. D. Gale, and M. C. Warren, *Phase Transitions* **61**, 141 (1997).
11. C. N. Chu, N. Saka, and N. P. Suh, *Mater. Sci. Eng.* **95**, 303 (1987).
12. L. L. Y. Chang, M. G. Scroger, and B. Phillips, *J. Am. Ceram. Soc.* **50**, 211 (1967).
13. J. Graham, A. D. Wadsley, J. H. Weymouth, and L. S. Williams, *J. Am. Ceram. Soc.* **42**, 570 (1959).
14. S. Y. Chang and S. J. Lin, *Scripta Mater.* **35**, 225 (1996).
15. *Smithells Metals Reference Book*, edited by E. A. Brandes and G. B. Brook (Butterworth-Heinemann Ltd., Oxford, 1992).
16. Wah-Chang, Zirconium Tungstate Property Sheet, 30 July 1996.
17. P. Atkins, *Physical Chemistry*, 5th ed. (Freedman, New York, 1994).
18. J. K. Lee, Y. Y. Earmme, H. I. Aaronson, and K. C. Russell, *Metall. Trans.* **11**, 1837 (1980).
19. M. A. Meyers and K. K. Chawla, *Mechanical Metallurgy Principles and Applications* (Prentice-Hall, Englewood Cliffs, NJ, 1984).
20. T. A. Hahn, in *Metal Matrix Composites: Mechanisms and Properties*, edited by R. K. Everett and R. J. Arsenault (Academic Press, Boston, 1991), p. 329.
21. P. S. Turner, *J. Res. Natl. Bur. Stand.* **37**, 239 (1946).
22. R. A. Schapery, *J. Comp. Mater.* **2**, 380 (1968).
23. E. H. Kerner, *Proc. Phys. Soc.* **69**, 808 (1956).
24. Y. L. Shen, A. Needleman, and S. Suresh, *Metall. Mater. Trans.* **25**, 839 (1994).
25. D. K. Balch, T. J. Fitzgerald, V. J. Michaud, A. Mortensen, Y. L. Shen, and S. Suresh, *Metall. Mater. Trans.* **27**, 3700 (1996).
26. Y. L. Shen, *Mater. Sci. Eng.* **237**, 102 (1997).
27. O. Sigmund and S. Torquato, *J. Mech. Phys. Solids* **45**, 1037 (1997).
28. S. Elomari, R. Boukhili, C. SanMarchi, A. Mortensen, and D. J. Lloyd, *J. Mater. Sci.* **32**, 2131 (1997).
29. S. Elomari, R. Boukhili, and D. J. Lloyd, *Acta Mater.* **44**, 1873 (1996).
30. D. C. Dunand and A. Mortensen, *Acta Metall. Mater.* **39**, 127 (1991).
31. *Metals Handbook: Properties and Selection: Nonferrous Alloys and Pure Metals* (American Society for Metals, Metals Park, OH, 1979).